

The effect of cross porting on derived displacement volume

Taeho Kim*, Paul Kalbfleisch* and Monika Ivantysynova*

Purdue University, Indiana, USA

Derived displacement volume (V_d) is very important for the calculation of volumetric and torque efficiency of positive displacement machines. A method for determining the derived displacement volume of a unit was introduced by Toet. This method is known to be more accurate than the current ISO 8426 standard, yet still has a speed dependent error. This paper reveals the main cause of the speed dependent error found in the method by Toet for the determination of derived displacement volume. An accurate pump model enabled the analysis of complex flow interactions inside a positive displacement machine. The analysis of the flows isolated the variations in derived displacement volumes to be dependent on the design of the valve plate. A case study of two valve plates with and without cross porting verified cross porting's influence on derived displacement volume. Steady state measurement and the pump model simulations at low pressure differences show that the effective displacement volumes (V_e) at different rotational speeds follow nonlinear curves that all converge at $\Delta p = 0$. The main cause of the speed dependent error of derived displacement volume calculated using the method by Toet was discovered as the change in back flow volume due to cross porting.

Keywords: derived displacement volume; derived capacity; cross port; axial piston machine; method by Toet; valve plate design

1. Introduction

Hydrostatic pumps and motors are widely used in many different industries due to their high power density and efficiencies. The determination of steady state performance characteristics of pumps and motors require their true displacement volume. The performance characteristics include the hydraulic-mechanical or torque efficiency and volumetric efficiency. The effective torque and effective outlet flow of a pump or motor can be directly measured under different steady state conditions detailed in ISO 4409. The corresponding torque and volumetric efficiencies can then only be determined using an accurate value for the displacement volume of the positive displacement machine.

The true displacement volume is defined as a derived displacement volume or derived capacity. There are two methods discussed in this paper for the determination of derived displacement volume. One is the method defined in ISO 8426, and the other is the method introduced by Toet (1970). The ISO method is characterized by measuring effective outlet flow at different rotational speeds at a constant pressure difference. The Toet method extrapolates the effective flow rate at the zero pressure difference point based on measurements of effective outlet flow at different pressures at a constant rotational speed.

The ISO 8426 method has pressure dependent errors, and the Toet method has speed dependent errors but is more accurate. The main source of speed dependent errors in Toet's method for calculating derived displacement has been discovered and will be explained in the remainder of this paper.

2. Valve plate design

Axial piston machines utilize a valve plate to facilitate the connections between the displacement chamber and the unit's suction and discharge ports. Consequently, the valve plate also defines the boundary between the two ports.

Fig. 1 shows a sketch of a valve plate for an axial piston machine. The rotation angle of the displacement chamber is shown as φ . The displacement chamber has its largest volume of fluid at the outer dead center (ODC) position and its smallest volume at the inner dead center (IDC) position. During pumping operations, the low pressure (LP) port is the suction port where flow comes into the displacement chamber. Similarly, the high pressure (HP) port is the discharge port where fluid is designed to flow from the displacement chamber.

The transitions from LP to HP (ODC areas) and vice versa (IDC areas) in the displacement chambers occur at these port boundaries, making the valve plate very important in the control of compression and expansion. The rise of displacement chamber pressure from suction to discharge is termed as compression. Similarly, fall in pressure from discharge to suction is termed expansion.

Research in the reduction of noise of pumps has motivated several techniques of designing valve plates to control the compression and expansion to decrease the audible noise generated by pumps and motors. Mainly, ideal timing and relief grooves are two design techniques that directly control the rates of compression and expansion.

Ideal timing will not be discussed in the paper, but more information can be found at Seeniraj (2009). Relief

*Corresponding authors. Email: kim1489@purdue.edu, pkalbfe@purdue.edu, mivantys@purdue.edu

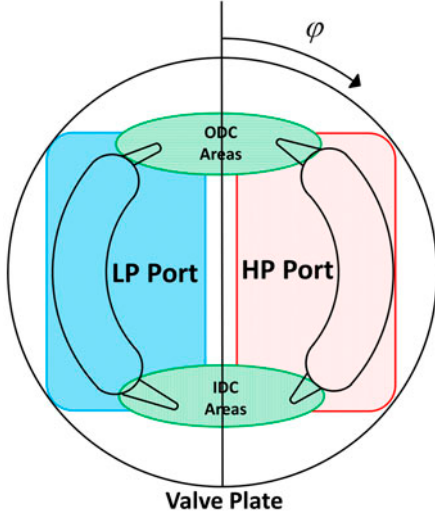


Fig. 1: Valve plate of an axial piston machine.

grooves are cuts made in the valve plate at the port boundaries that create small openings between the ports and the displacement chamber. This enables smaller amounts of fluid to flow between the fluid volumes during compression and expansion. This, in turn, allows for a greater amount of control of the displacement chamber pressure.

It is very common for relief groove designs to allow, for a few degrees, the displacement chamber to be connected to both ports at the same time. During that time, some HP fluid will flow back into the displacement chamber, and similarly some displacement chamber fluid will flow into the LP port. This process is called cross porting because it allows some fluid to flow from one port through the displacement chamber into the other port.

The flow behavior during the cross port region is complex due to the interactions of several fluid flows simultaneously. This makes it very hard to measure and analyze the effect cross porting has on a specific valve plate design. However, the effect of cross porting can be analyzed by modeling the flow through an axial piston machine. This modeling technique used for this research study is based on Wieczorek and Ivanysynova's (2000) lumped parameter model.

3. Pump modeling

The pump model simulates the individual flow of all the displacement chambers to and from both the HP port and LP port. These complex interactions of fluid flows during the cross port region can be determined explicitly.

The instantaneous displacement chamber pressure, within the pump model, is calculated in each displacement chamber using the pressure build up Eq. 1 by summing all the flows entering and exiting a control volume depicted in Fig. 2.

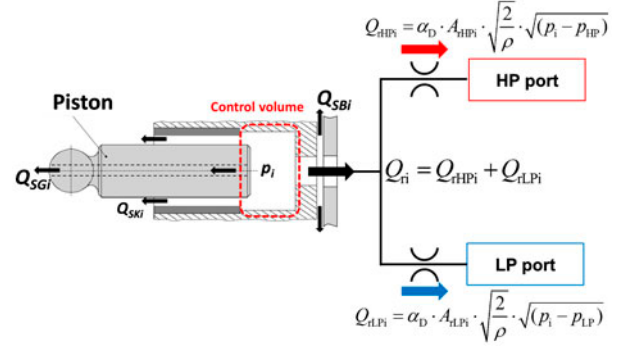


Fig. 2: Flows at a single displacement chamber.

$$\frac{dp_i}{dt} = \frac{K}{V_i} \left(Q_{ri} - Q_{SKi} - Q_{SBi} - Q_{SGi} - \frac{dV_i}{dt} \right) \quad (1)$$

Q_{SKi} represents the leakage flow rate between each piston and cylinder. Q_{SBi} represents the leakage flow rate between the cylinder block and valve plate. Q_{SGi} represents the leakage flow rate through the piston bore to the slipper. Q_{SKi} , Q_{SBi} , and Q_{SGi} are set to 0 to exclude the effect of external leakages. Q_{ri} represents the volumetric flow into a single displacement chamber and is calculated by summing the fluid flow between the displacement chamber and the each port, shown in Eq. 2:

$$Q_{ri} = Q_{rHPi} + Q_{rLPi} \quad (2)$$

Q_{rHPi} represents the volumetric flow from a single displacement chamber to the HP port. Q_{rLPi} represents the flow to a single displacement chamber from the LP port as described in Fig. 2. Both flows are assumed to be turbulent and are modeled using the orifice equation.

Fig. 3 shows the flow between a single displacement chamber and the HP and LP ports, Q_{rHPi} and Q_{rLPi} , for one shaft revolution respectively. A positive flow represents fluid flowing into the displacement chamber, and a

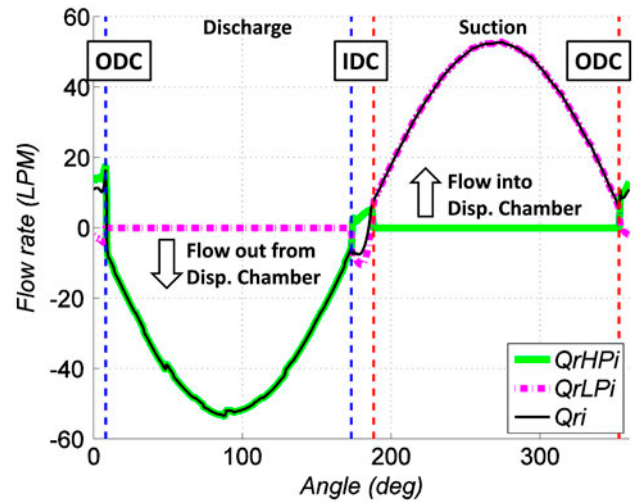


Fig. 3: Instantaneous volumetric flow of a single piston.

negative flow represents fluid flowing out of the displacement chamber.

The discharge flow (Q_{rHP}) can be calculated from the summation of all the individual flows of all displacement chambers to the HP port (Q_{rHPi}).

$$Q_{rHP} = \sum_{i=1}^z Q_{rHPi} \quad (3)$$

4. Power losses in positive displacement machines

4.1 Displacement volumes

In general, there are several ways to define the term “displacement volume.” Displacement volume is the maximum change of displacement chamber volume during one revolution of the shaft.

Displacement volume can be differentiated more precisely as geometric displacement volume (V_g), effective displacement volume (V_e), and derived displacement volume (V_i). Geometric displacement volume (V_g) is calculated volume from the geometry of the displacement chamber. Effective displacement volume (V_e) is the quotient of the effective flow rate (Q_e) by the rotational speed (n). Derived displacement volume (V_i) is only determined from the steady state measurement of the effective flow rate and rotational speed at multiple operating conditions (Ivantysyn and Ivantysynova, 2003). Derived displacement volume is used for the calculation of volumetric and torque efficiency.

4.2 Type of power losses

Power losses in positive displacement machines can be divided into volumetric losses (Q_s) and hydromechanical (torque) losses (T_s). Some of the input energy is transferred into heat due to the flow in the lubricating gaps existing between the relatively moving parts of the pump. Volumetric losses (Q_s) are defined as the difference between theoretical outlet flow and effective volumetric flow. Similarly, hydromechanical (torque) losses (T_s) are defined by the difference between effective torque and theoretical torque. The effective outlet flow of a pump is reduced due to gap flows, cross port flow, and the compressibility of fluid. The effective torque of a pump is increased compared to the theoretical torque through the amount of torque necessary to overcome friction and pressure drop in pump cavities connecting the displacement chamber with pump ports.

Volumetric losses (Q_s) and hydromechanical losses (T_s) can be expressed as Eqs. 4 and 5:

$$Q_s = V_i \cdot n - Q_e \quad (4)$$

$$T_s = T_e - \frac{V_i \cdot \Delta p}{2\pi} \quad (5)$$

Volumetric losses (Q_s) and hydromechanical losses (T_s) can only be calculated, from steady state

measurements, knowing the derived displacement volume (V_i). Volumetric efficiency, hydromechanical efficiency, and total efficiency are defined in Eqs. 6–8:

$$\eta_v = \frac{Q_e}{n \cdot V_i} \quad (6)$$

$$\eta_{hm} = \frac{T_i}{T_e} = \frac{V_i \cdot \Delta p}{2\pi \cdot T_e} \quad (7)$$

$$\eta_t = \frac{P_{out}}{P_{in}} = \frac{Q_e \cdot \Delta p_i}{T_e \cdot \omega_i} = \eta_v \cdot \eta_{hm} \quad (8)$$

Derived displacement volume (V_i) is therefore crucial for calculating the volumetric efficiency and hydromechanical efficiency.

5. Methods for V_i determination

Two methods are often used for the determination of derived displacement volume: one is the method defined in ISO 8426 (Fig. 4), and the other is the method by Toet (Fig. 5).

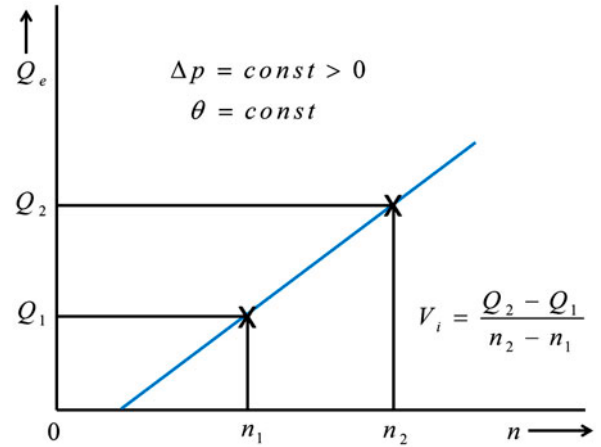


Fig. 4: V_i from method defined in ISO 8426.

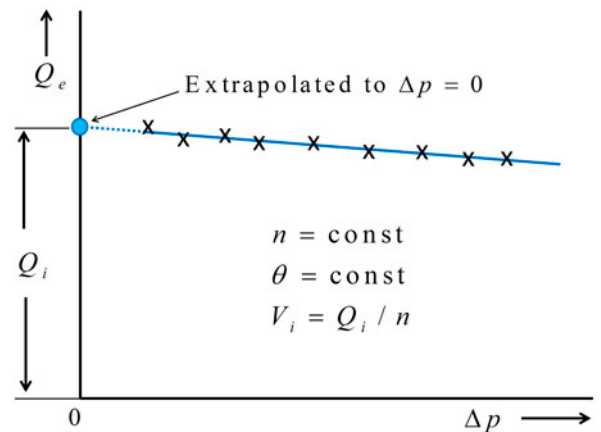


Fig. 5: V_i from method by Toet.

5.1 V_i from method defined in ISO 8426

Ideally, the derived displacement volume needs to be measured at zero pressure difference because, at this point, the pump will have zero volumetric losses. In real measurement conditions, derived displacement volume is often measured at different pressure differences with the lowest Δp often being larger than 0. In case the lowest pressure difference is not 0, pressure dependent errors will be introduced due to volumetric losses.

The method defined in ISO 8426 uses measurements of effective outlet flow rate at different speeds at a constant pressure and constant input fluid temperature. The derived displacement volume can be determined by Eq. 9.

$$V_i = \frac{Q_2 - Q_1}{n_2 - n_1} \quad (9)$$

where Q is the effective flow rate and n is the rotation speed of a pump.

The derived displacement volume (V_i) defined in ISO 8426 (Eq. 9) changes while measuring along multiple pressure differences. This makes the derived displacement volume calculation inaccurate.

5.2 V_i from method by Toet

In the method by Toet, the effective flow rate is measured at different pressure differences at a constant speed. The derived displacement volume is determined by the extrapolation of the effective flow rate to a point where $\Delta p = 0$ (Eq. 10):

$$V_i = \frac{Q_i}{n} \quad (10)$$

Q_i is the flow rate extrapolated to a point where $\Delta p = 0$ and n is the rotational speed of a pump.

The merit of the method by Toet is that the measured values for the efficiency test can be used for determination of derived displacement volume without additional measurements. The demerit of the method by Toet is that the derived displacement volume is different with varying speed settings. Both methods have problems because both methods create different values for derived displacement volume for different operating conditions. The ISO method creates different values of the derived displacement volume for different pressures, and the method by Toet creates different values of the derived volume for different speeds. Therefore, it is difficult to decide which method should be used. More discussion on this topic can be found in Post (1996). The authors' research group has used the method by Toet for decades. This research study reveals one of the main reasons for the speed dependent error in the derivation of the derived displacement volume when applying the method by Toet.

5.3 Demerit of the method by Toet

For the convenience of analysis, effective displacement volume is plotted directly instead of the effective flow

rate (Fig. 6). Fig. 6 shows the derived displacement volume (y -intercept) determined using the method by Toet from a steady state measurement of a 75cc pump. The pressure difference, rotational speed, effective flow rate, case flow, effective torque, and fluid temperatures were measured.

In the measurement, one can observe that the derived displacement volume increases with the rotational speed (Fig. 6). The reason for this speed dependent error of the derived displacement volume in the method by Toet was not known. To correct this speed dependent error, an average value of the derived displacement volumes is often used in practical applications, or different values of V_i are used for different speeds.

When calculating the effective displacement volume (V_e) using Eq. 12, it can be seen that the effective displacement volume increases with rotational speeds also in measurement as shown in Fig. 6.

5.4 V_e determined from simulation and measurement

The simulation model described in Section 3 allows for the analysis of the individual flow for each displacement chamber, which sum together to form the effective flow rate. Therefore, the physical behavior of the speed dependent error of the derived displacement volume in the method by Toet can be analyzed. The effective flow rates and the derived displacement volumes are calculated from Eq. 13 and are linearly extrapolated to a point where $\Delta p = 0$ (Fig. 7).

The pump model considers steady state conditions. This enables the simulated discharge flow rate (Q_{rHP}) to represent the effective flow rate (Q_e) of a real unit measured under steady state conditions. One important difference between Q_{rHP} and Q_e is the intentional exclusion of external leakages in Q_{rHP} .

$$Q_{rHP} \approx Q_e \quad (11)$$

The effective displacement volume can be calculated using Eq. 12:

$$V_e = \frac{Q_e}{n} \quad (12)$$

Combining Eqs. 11 and 12, the effective displacement volume can be calculated from the flow Q_{rHP} using Eq. 13:

$$V_e = \frac{Q_{rHP}}{n} \quad (13)$$

The V_e calculation is repeated for different rotational speeds. The V_i can then be determined from linearly extrapolating the V_e along constant rotational speed to the point where $\Delta p = 0$ (Fig. 7).

For this research study, a single 75cc unit was both measured and simulated at the same operating conditions. Notice the speed dependent error is captured in simulation without the need to model complex physical phenomenon of gap flow, which would be required in order to calculate the external leakages.

The speed dependent error of V_i in the method of Toet is more prominent at low rotational speeds than high speeds. The speed dependent errors become smaller as the rotational speed increases. The rotational speed ranges are determined to show the speed dependent error changes, which in our case range from 500 to 2000 rpm.

5.5 V_i determined from simulation and measurement

The extrapolated V_i are calculated from both simulated and measured V_e (Figs. 6 and 7). Fig. 8 shows the multiple V_i corresponding to the four different rotational speeds analyzed.

Derived displacement volumes (V_i) determined from the steady state measurement and the simulation have a similar trend of increasing with speed (Fig. 8). The higher value of the derived displacement volume from simulation can be explained through the small deviation of design parameters and the exclusion of external

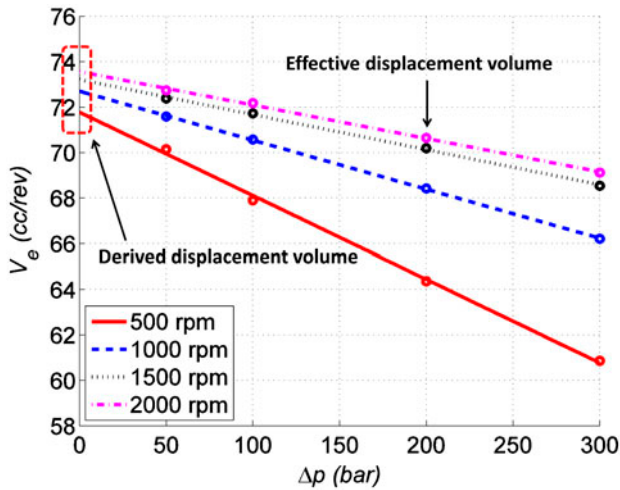


Fig. 6: V_i from the steady state measurement using the method by Toet (75cc pump).

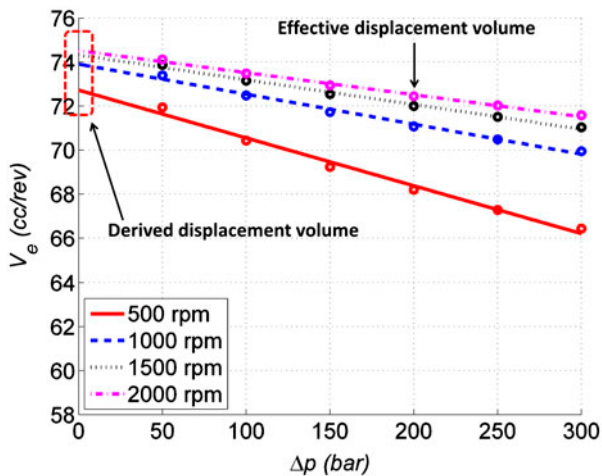


Fig. 7: V_i obtained from the pressure module simulation using the method by Toet (75cc pump).

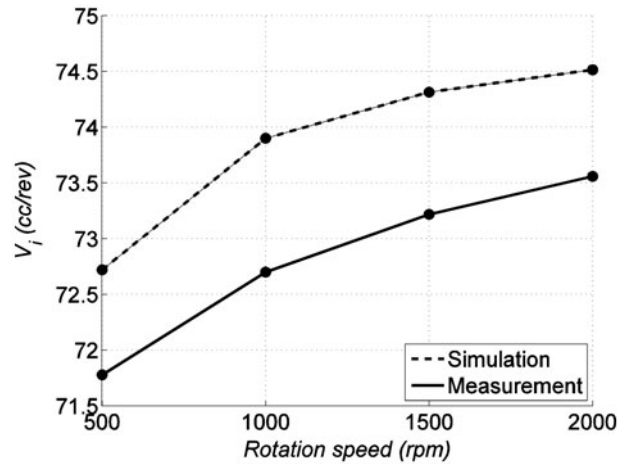


Fig. 8: Comparison of V_i determined from simulation and measurement for different speeds.

leakages from the simulation. The small deviation of design parameters, like piston diameter and maximum swash plate angle of the real unit, used for steady state measurements differ from all the nominal design parameters used in simulations. As a comparison, V_i determined from theoretical flow rate is constant across all rotational speeds.

This similar trend of the speed dependent error in the derived displacement volume between the measurements and the simulations shows that the pump model simulations capture the physics of the speed dependent error in the method by Toet. The pump model has been used to investigate what causes this speed dependent error.

6. Flow rate analysis

6.1 Flow rate analysis for a single displacement chamber

Fig. 9 shows the discharge flow (Q_{rHPi}) of a single piston during one revolution. The cross port regions at

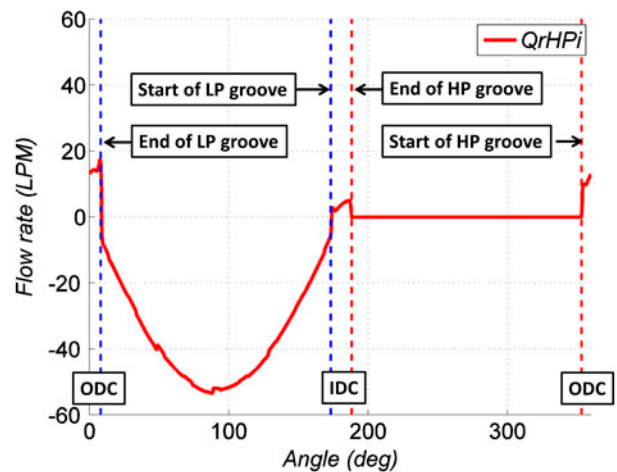


Fig. 9: Discharge flow of a single displacement chamber.

ODC and IDC are represented between the two dashed lines in Fig. 9. The positive flow in Fig. 9 represents flow from the HP port to displacement chamber. The negative flow in Fig. 9 represents flow from the displacement chamber to the HP port. The positive flow at the ODC and IDC regions represents back flow into the displacement chamber at the cross port regions.

6.2 Single piston effective displacement volume (V_{ei})

The single piston effective displacement volume (V_{ei}) is defined to analyze the effect of the flow from a single displacement chamber. V_{ei} is defined as the quotient of effective displacement volume (V_e) and the number of piston (z) (Eq. 14).

$$V_{ei} = \frac{V_e}{z} \quad (14)$$

The single piston effective displacement volume (V_{ei}) can also be calculated by integrating the discharge flow of a single displacement chamber over the time of one revolution (Eq. 15).

$$V_{ei} = \int_{t=t_{\phi=0}}^{t=t_{\phi=360}} Q_{rHPi} dt \quad (15)$$

It is convenient to separate the integration (Eq. 15) into three mutually exclusive regions (Eq. 16 and Fig. 10).

$$\begin{aligned} V_{ei1} &= \int_{t=t_{\phi_{HP}start}}^{t=t_{\phi_{LP}end}} Q_{rHPi} dt \\ V_{ei2} &= \int_{t=t_{\phi_{LP}end}}^{t=t_{\phi_{LP}start}} Q_{rHPi} dt \\ V_{ei3} &= \int_{t=t_{\phi_{LP}start}}^{t=t_{\phi_{HP}end}} Q_{rHPi} dt \end{aligned} \quad (16)$$

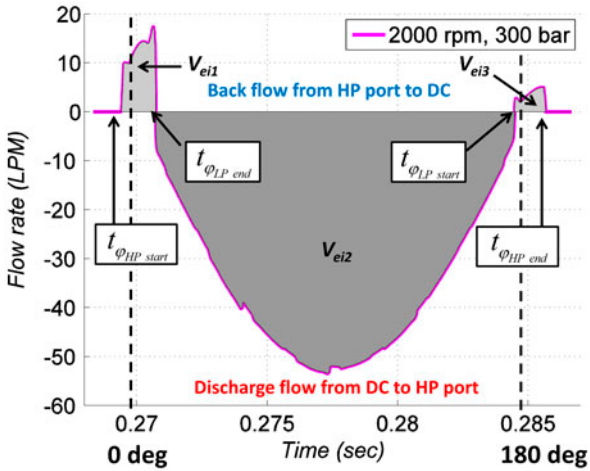


Fig. 10: Calculation of the single piston effective displacement volume (V_{ei}).

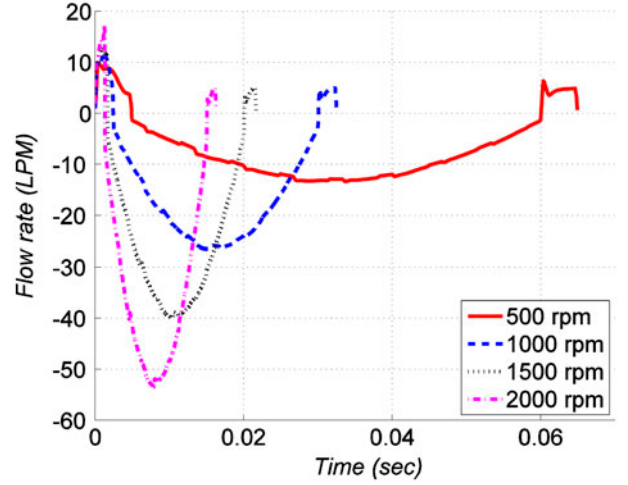


Fig. 11: Simulated discharge flow Q_{rHPi} of a single displacement chamber for different rotational speeds.

V_{ei1} is the fluid volume during the ODC cross port region, mostly from the HP port to the displacement chamber. V_{ei2} is the fluid volume between ODC and IDC regions mostly discharged to the HP port. V_{ei3} is the fluid volume during the IDC cross port region, mostly from the HP port to the displacement chamber.

Therefore, the cross port back flow volume (V_{bfi}) is defined as the volume flow into a displacement chamber during both cross port regions (Eq. 17).

$$V_{bfi} = |V_{ei1}| + |V_{ei3}| \quad (17)$$

Fig. 11 shows the discharge flow of a single displacement chamber (Q_{rHPi}) for one revolution for four different rotational speeds at a pressure difference of 300 bar. Notice the time for one revolution decreases and the discharge flow rate increases as the rotational speed of a pump increases.

The single piston effective displacement volume (V_{ei}) and cross port back flow volume (V_{bfi}) are calculated by integrating the discharge flow over one shaft revolution.

6.3 The cross port effect on V_i

Fig. 12 shows the values of the single piston effective displacement volumes (V_{ei}) at different rotational speeds. The single piston effective displacement volume (V_{ei}) increases as rotational speed increases.

Fig. 13 compares the V_{ei} with its components V_{ei2} and V_{bfi} while using two axes for convenience. Reference the right axis for V_{bfi} .

The fluid volume between the ODC and IDC regions (V_{ei2}) remains constant with changes in rotational speed.

$$V_{ei2} \approx \text{constant} \quad (18)$$

The cross port back flow volume (V_{bfi}) decreases as rotational speed increases (Fig. 13). Organizing the total V_{ei} into V_{ei2} and V_{bfi} makes the cause of V_{ei} change due to rotational speed apparent.

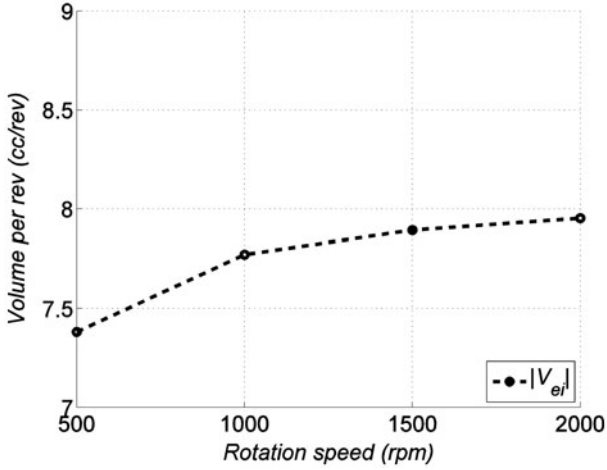


Fig. 12: Single piston effective displacement volume at different rotational speeds.

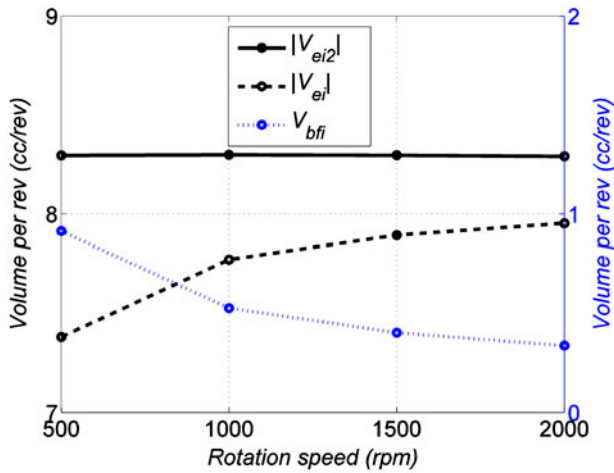


Fig. 13: Single piston cross port back flow volume (V_{bfi}) at different rotational speeds.

$$V_{ei} = \underbrace{|V_{ei2}|}_{\approx \text{constant}} - V_{bfi} \quad (19)$$

Therefore, as seen in Fig. 13, any increase in V_{ei} is accompanied with a decrease in V_{bfi} . Fig. 13 illustrates the strong negative correlation between V_{ei} and V_{bfi} .

It is shown that the cross port back flow volume decreases as rotational speed increases. This decrease of the cross port back flow leads to the increase of the effective displacement volume and the derived displacement volume.

6.4 V_i without cross port

To verify the influence of the cross port back flow on the derived displacement volume (V_i), a design without the cross port was modeled. The orifice areas in the

cross port regions were removed to eliminate the effect of cross porting (Fig. 14).

The derived displacement volume (V_i) calculated using the pump model simulation with a valve plate without cross port for different speeds is shown in Fig. 15. Notice that without cross port, the effective displacement volume (V_e) does not increase as the rotational speed increases. Similarly, the derived displacement (V_i) does not increase either. Fig. 15 shows that all the effective displacement volumes at each pressure difference coincide and therefore are graphed as a single point. Furthermore, all the linearly extrapolated lines appear to be a single line.

From Fig. 15, it is clear that the speed dependent error of the method by Toet is not existing for valve plates without cross port. The comparison of the derived displacement volume between simulations with and

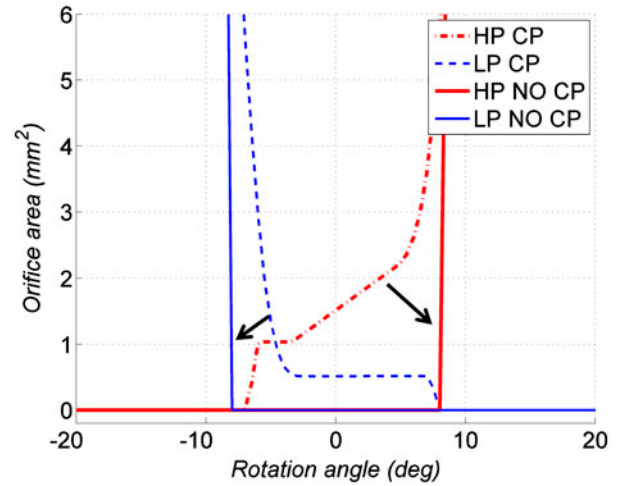


Fig. 14: The original valve plate orifice area (dashed line) vs. the modified valve plate orifice area (solid line).

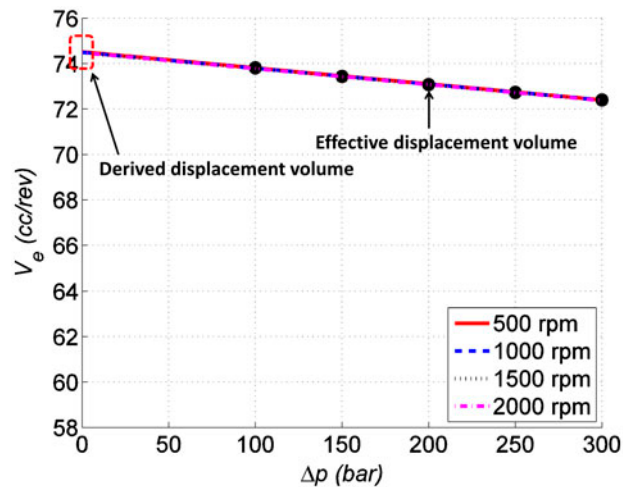


Fig. 15: Calculation of V_i for a valve plate without cross port.

without cross porting shows that the speed dependent error of the derived displacement volume (V_i) in the method by Toet is caused by the cross port.

6.5 V_i at small pressure difference

The model was used to study the behavior at 0, 10, 20, 30, 40, and 50 bar pressure differences to check the effect of cross porting at small pressure differences. The effective displacement volumes (V_e) were calculated at each pressure difference. As the pressure difference gets smaller, the effective displacement volumes (V_e) converge at $\Delta p = 0$ to a single displacement volume (Fig. 16).

Steady state measurements were conducted on the same 75cc unit at the same small pressure difference conditions. The tendency of the measured effective displacement volumes (V_e) is similar to the simulations.

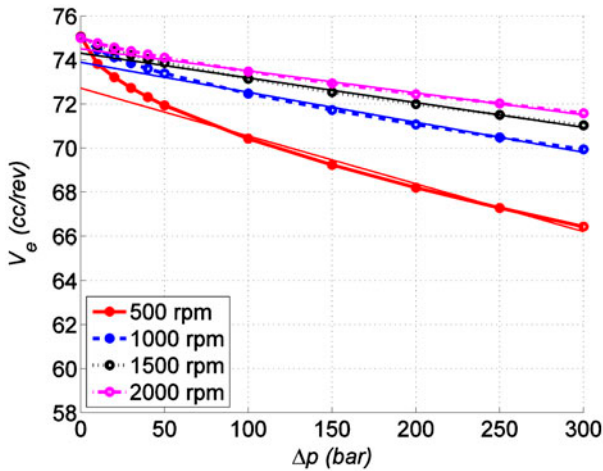


Fig. 16: V_e from small pressure difference simulation.

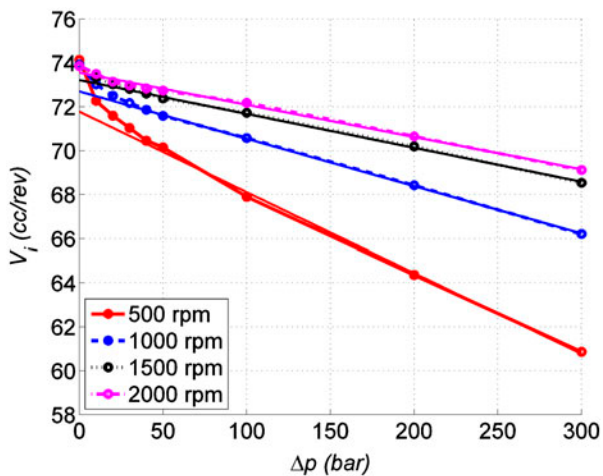


Fig. 17: V_e from small pressure difference measurement.

Both simulated and measured effective displacement volumes converge at $\Delta p = 0$ with all curves being non-linear (Figs. 16 and 17). It can be seen from Figs. 16 and 17 that using very low values of pressure difference for a pump with cross port will help to improve the accuracy of the determination of the derived displacement volume (V_i). The value of V_i determined from simulation is very close to the value determined from measurement. The difference of 1cc can be explained by the deviation of real geometry (design parameters) of the real unit from the nominal geometry used in simulation and the exclusion of external leakages from the simulation. For example, a small change of the maximum swash plate angle is sufficient to eliminate the differences.

7. Conclusion

Steady state measurements were conducted at various rotational speeds and pressures using a 75cc unit. The calculation of the derived displacement volume (V_i) using the pump model correlates well with measurements. The pump model calculated flows from a single displacement chamber, which cannot be measured directly from steady state measurements. The discharge flow rate from a single piston for one revolution was integrated and analyzed to investigate the reason for the speed dependent error found in the method of Toet for the determination of derived displacement volume.

A comparison of two valve plates, with and without cross porting, verified the influence cross porting has on the speed dependent error of the method by Toet. In the case without cross porting, all the effective displacement volumes at each pressure difference coincided to a single point. Therefore, no speed dependent error is observed for valve plates without cross porting.

The effective displacement volumes (V_e) were calculated from both steady state measurements and simulations at small pressure differences. Both simulations and measurements at small pressure differences show that the effective displacement volumes (V_e) at different rotational speeds follow nonlinear curves, which all converge at $\Delta p = 0$.

The back flow due to a cross port design of the valve plate has been discovered as the source of the speed dependent error of the method by Toet for determining the derived displacement volume. An increase in rotational speed will cause less back flow through cross porting. The nonlinearity of cross port flow results in multiple derived displacement volumes when using the method by Toet.

Therefore, it is recommended to conduct steady state measurements also at the smallest pressure differences possible, in order to keep the speed dependent error very small for all units with a cross port. Also it is recommended to use the highest rotational speed to determine the derived displacement volume because of the more linear behavior.

Nomenclature

A	Valve plate orifice area	m^2
Q_s	Volumetric losses	m^3/s
Q_e	Effective flow rate	m^3/s
Q_{rHP}	Flow rate to HP port	m^3/s
Q_{rLP}	Flow rate to small pressure port	m^3/s
Q_{SK}	Flow rate between piston and cylinder	m^3/s
Q_{SB}	Flow rate between cylinder block and valve plate	m^3/s
Q_{SG}	Flow rate through the bore of the piston to the slipper	m^3/s
z	Number of piston	—
T_i	Input torque	Nm
T_s	Torque losses	Nm
T_e	Effective torque	Nm
V_g	Geometric displacement volume	m^3
V_e	Effective displacement volume	m^3
V_i	Derived displacement volume	m^3
V_{bf}	Back flow volume	m^3
p	Pressure	Pa
η_v	Volumetric efficiency	—
η_{hm}	Hydromechanical efficiency	—]
η_t	Total efficiency	—
φ	Angle	deg
P_{in}	Input power	W
P_{out}	Output power	W
θ	Temperature	$^{\circ}\text{C}$
K	Bulk modulus of fluid	Pa
ρ	Fluid density	kg/m^3
n	Rotational speed	rpm

Notes on Contributors



Taeho Kim Born on March 18, 1981, in Busan (South Korea). He received his BS degree from Ajou University and MS degree from KAIST, South Korea, and University of Florida, in Mechanical Engineering in 2012. He is currently a PhD student at Maha Fluid Power research center. His main research interests are noise and control of displacement machines and quiet fluid power systems.



Paul Kalbfleisch Born on November 20, 1988, in Louisville, Kentucky. He received his BS degree in Engineering in Acoustics from Purdue University in 2011. He is currently a master's student in Mechanical Engineering at Purdue University. His main

research interests are modeling and design of hydraulic pumps/motors and transmissions for the purpose of noise reduction.



Monika Ivantysynova Born on December 11, 1955, in Polenz (Germany). She received her MSc degree in Mechanical Engineering and her PhD degree in Fluid Power from the Slovak Technical University of Bratislava, Czechoslovakia. After 7 years in the fluid power industry, she returned to university. In April 1996, she received a Professorship in fluid power and control at the University of Duisburg (Germany). From 1999 until August 2004, she was Professor of Mechatronic Systems at the Technical University of Hamburg-Harburg. Since August 2004, she has been a Professor at Purdue University. Her main research areas are energy saving actuator technology and model based optimization of displacement machines, as well as modeling, simulation, and testing of fluid power systems. Besides the book *Hydrostatic Pumps and Motors* published in German and English, she has published more than 80 papers in technical journals and at international conferences.

References

- International Standard, 1988. *Hydraulic fluid power—positive displacement pumps and motors—determination of derived capacity*. ISO: International Organization for Standardization 8426.
- International Standard, 1986. *Hydraulic fluid power—positive displacement pumps, motors and integral transmissions—determination of steady-state performance*. ISO: International Organization for Standardization 4409.
- Ivantysyn, J. and Ivantysynova, M., 2003. *Hydrostatic pumps and motors, principles, designs, performance, modeling, analysis, control and testing*. New Delhi: Academic Books International.
- Post, W.J.A.E.M., 1996. Models for steady-state performance of hydraulic pumps: determination of displacement. *9th Bath International Fluid Power Workshop*, University of Bath, UK, Vol. 9, p. 339.
- Seeniraj, G.K., 2009. *Model based optimization of axial piston machines focusing on noise and efficiency*. Thesis (PhD). Purdue University.
- Toet, G., 1970. Die Bestimmung des theoretischen Hubvolumens von hydrostatischen Verdrängerpumpen und Motoren aus volumetrischen Messungen. *Ölhydraulik und Pneumatik* 14. Nr: 5, 185–190.
- Wieczorek, U. and Ivantysynova, M., 2000. *Caspar—a computer-aided design tool for axial piston machines*. Proceedings of the Bath Workshop on Power Transmission and Motion Control: University of Bath, UK, 113–126.